Thermal fatigue behavior of functionally graded W/EUROFER-layer systems using a new test apparatus

Thomas Emmerich[a,1], Robert Vaßen[b], Jarir Aktaa[a]

[a]*Karlsruhe Institute of Technology (KIT), Institute for Applied Materials, Hermann-von-Helmholtz-Platz 1, 76344 Eggenstein-Leopoldshafen, Germany*

[b]*Forschungszentrum Jülich GmbH (FZJ), Institute of Energy and Climate Research, Wilhelm-Johnen-Straße, 52425 Jülich, Germany*

In future fusion reactors tungsten coatings shall protect First Wall components, made of reduced activation ferritic martensitic steel, against the plasma, because of tungsten's favourable thermo-mechanical properties and low sputtering yield. Functionally graded material layers implemented between the coating and the steel substrate, compensate the difference in the coefficient of thermal expansion. By using the vacuum plasma spraying technique several layer systems were successfully produced and tested, among other aspects, in regard to their thermal fatigue behaviour up to 500 thermal cycles in a vacuum furnace. However, higher numbers of thermal cycles are anticipated for future fusion reactors and, therefore, a less time consuming approach for thermal fatigue testing is required.

Hence, a new testing apparatus with induction heating and inert gas cooling was built and first thermal fatigue experiments with up to 5000 cycles were carried out on different functionally graded tungsten/steel layers systems. The subsequent investigations of these samples show that the layer systems are stable for the applied number of thermal cycles and their properties are solely determined during their respective coating processes.

[1] Corresponding author E-mail:thomas.emmerich@kit.edu

Keywords: *tungsten, first wall, functionally graded material (FGM), vacuum plasma spraying, thermal fatigue*

1. Introduction

To protect First-Wall (FW) structures of future fusion power plants it is considered to use tungsten (W) coatings, because of its favorable thermo-mechanical properties and low sputtering yield. By using functionally graded (FG)-layer systems between the W-coating and steel substrate, made out of a reduced activation ferritic martensitic steel like EUROFER, the difference in the coefficient of thermal expansion (CTE) can be compensated [1]. Respective layer systems, with three- or five-step FG-layers and a W-top coat, were successfully deposited on EUROFER substrates in previous experiments by the vacuum plasma spraying (VPS) technique [2,3]. The coatings have a total thickness in the range of 800 to 1200 μm [2,3] and exhibit at 550 °C satisfactory adhesion and indications of metallurgical bonding to the substrate [3]. In regard to the layers thermal behavior, tests show that the layers resist thermal shocks of at least 0.19 GW/m² and are not damaged by 500 cycles of thermal fatigue between 350 and 550 °C in a vacuum furnace [3,4].

A further increase of coating thickness, with 1.2 mm thick FG-layers and a 0.8 mm thick W-top coat, was also successfully achieved [3,4]. 1.2 mm or thicker FG-layers are preferred, because finite element (FE)-simulations indicate that then the maximum creep strain per thermal cycle in the EUROFER substrate is significantly reduced [1]. Furthermore, it was shown on three additional coatings, consisting only of 700 μm thick FG-layers, that the VPS induced substrates hardness loss can be moderated by using modified spraying parameters [3,4]. The hardness loss occurs, when during coating the substrate temperature exceeds the materials tempering temperature, what leads to grain growth [3] or may even destabilize the ferritic martensitic (FM)-microstructure. The adhesion of these four layer systems was investigated by fracture mechanical tests and the results indicate

that, except for the coating produced with increased spraying distance, interface toughness values and metallurgical bonding like in the previous layer systems were achieved [5].

Due to these encouraging results, the thermal fatigue behavior of the coatings is of interest: in case of the thicker coating particularly in regard to thermal cycles expected for future fusion reactors [6], and in case of the coatings produced with modified spraying parameters, whether the modified spraying affects the thermal fatigue behavior. To achieve high cycle numbers in a reasonable testing time, the thermal fatigue tests were not conducted in a vacuum furnace [3] but in a new thermal fatigue testing apparatus.

2. Experimental

2.1. Testing setup

In previous thermal fatigue tests, performed in a vacuum furnace, heating and cooling were time consuming with durations of about 1000 s and 2900 s, respectively [3]. To achieve a high number of thermal cycles in a test time as short as possible a new testing apparatus was constructed. Figure 1 depicts a schematic sketch of its testing chamber.
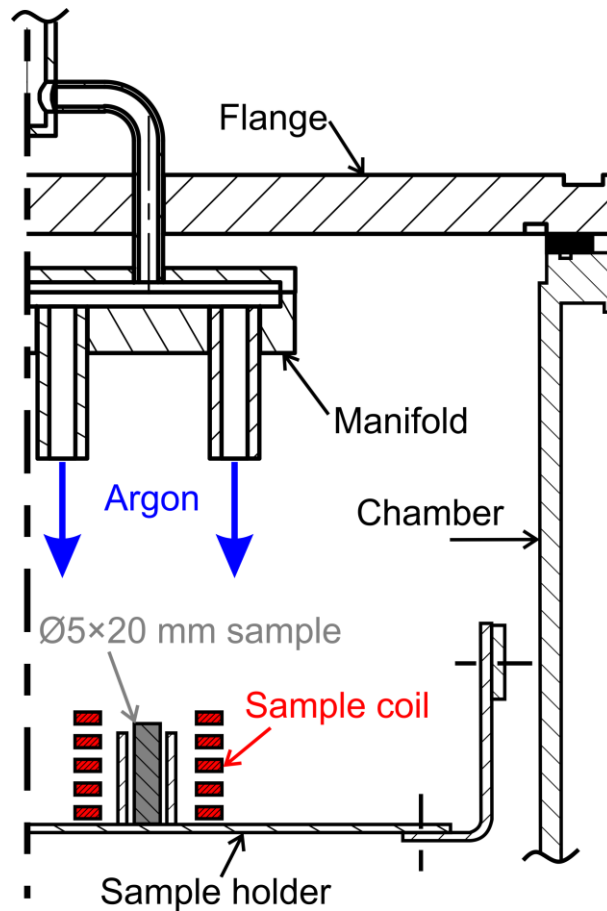
Figure 1. Schematic cross-section of a part of the apparatus testing chamber.

The testing chamber consists out of a cylindrical stainless steel vessel and is closed with a flange, with ISO-sealing, on top. For heating an induction heating system is utilized, which has a maximum output of 1.5 kW. The whole induction coil is of special design and consists of two, smaller sample coils, so that two cylindrical samples can be tested at the same time. The sample temperatures are monitored with two pairs of Ø0.3 mm NiCr/Ni-wires (Type-K thermocouples), attached by spot-welding to the samples, and a precision of two decimal places. The samples are mounted constrain free on the sample holder and kept in place by small cylinders and a slight pressure by the thermocouple-wires. Both the holder and the cylinders are made of a glass/ceramic-compound material, which is not affected by the induction heating. Hence, neither heating power is lost nor unnecessary heating occurs. Furthermore, the material withstands the desired fast heating and cooling rates. The sample holder itself is fixed to the chamber walls by

4

steel fastener. To suppress oxidation of the samples during testing, the gas volume inside the closed chamber is exchanged beforehand by Argon (Ar), with a purity of 99.999 %, about five-times the chambers volume. The gas is supplied from the top and distributed by the manifold above each sample into four tubes that are arranged concentrically around each sample coil. Ar is also used for cooling the samples, by streaming fresh Ar into the chamber, while the induction heating is switched off. Backflow of gas or ingress of air are prevented by a check valve, which opens at a pressure of 0.07 bar, in the outlet tube. Accordingly, samples made of EUROFER exhibited after testing generally no noticeable oxide layers.

For the temperature control of the experiment, utilizing PI-elements in the software LabView, the instantaneous sample temperatures are used, which are primarily determined close to the samples substrate/coating interface. In case only one sample is tested in the facility, the second thermocouple is attached to the sample center lengthwise. To ensure that the desired maximum and minimum temperature are achieved, the actual lowest and highest temperature is taken for the system control, respectively.

2.2. Tested coating systems

Thermal fatigue tests were performed on the layer systems listed in Table 1. On layer system 1 the complete coating, consisting of a 1.2 mm thick, five-stepped FG-layer and a 0.8 mm thick W-top coat, was successfully deposited, while on layer system 2 to 4 the influence of modifying the spraying parameters was tested by a 700 μm thick FG-layer. The resulting substrate hardness profiles are plotted in Figure 2 . Layer system 3 and 4 show hardness losses after coating, which occurs when the nominal substrates tempering temperature is exceeded during coating, causing grain growth [3], whereas layer system 2 exhibits no change in the substrate hardness due to the greater spraying distance. On the other hand, layer system 1 displays a hardness increase close to the coating/substrate interface, followed by a hardness decrease at a distance of around

2.5 mm from the interface. The cause for this effect shall also be addressed in this paper. In view of the layer systems thermal fatigue behavior, the thermal stresses will be higher in layer system 1 than in the three other systems, due to its thicker coating with a W-top coat. Nonetheless, thermal stresses still exist in system 2 to 4 and may affect, together with the modified spraying parameters, the coating adhesion.

The layer systems were tested in form of cylindrical samples with dimensions of about Ø5×20 mm. Such thick substrate material (18 mm), compared to the amount of layer material (0.7 up to 2 mm), subdues the deformation of the samples and thus also relief of residual stresses, allowing a more conservative testing of the layer system. The cylindrical samples were produced by electrical discharge machining from the coated plates with a tolerance of $Ø5_{-0.1}^{+0}$ mm and the oxide surface layer was removed by grinding (1200 grit paper), so that the thermocouple-wires could be attached.

Table 1. List of tested layer systems [4,5,7,8].

| Layer system number	Ratio W/EUROFER in % of layer	Nominal layer thickness in µm	Spraying parameters	Number of tested cycles
1	25/75	240	Standard spraying parameters	
	37/63	240	Preheating to about 700 °C	
	50/50	240	Plasma current: 750 A	
	63/37	240	Spraying distance: 0.3 m	
	75/25	240	Movement speed of spraying	
	100/0	800	system: 0.44 m/s	250
				500
2	25/75	700	Preheating to about 600 °C Spraying distance: 0.4 m	1000
				2000
				5000
3	25/75	700	Preheating to about 600 °C Plasma current: 700 A	
4	25/75	700	Preheating to about 700 °C Movement speed: 0.5 m/s	

6
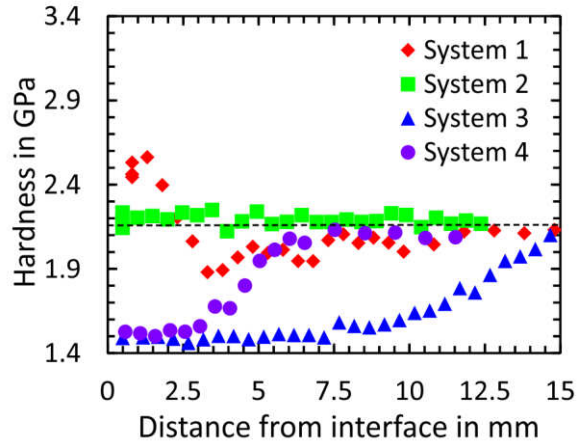
Figure 2. Substrate hardness profiles after coating [4] with the nominal hardness of EUROFER marked by the dashed line.

2.3. Testing and evaluation procedures

To achieve the thermal cycling maximal 8 % of the induction system power is applied for heating and for cooling a volume stream of 5 l/min is let through. In this way, heating and cooling rates higher than 8 °C/s and 4 °C/s are attained, respectively. Because of these much higher rates than in the vacuum furnace [3], the lower temperature limit was extended to 300 °C, i.e. the minimum coolant inlet temperature for the blanket [9,10], realizing thermal cycles that are more conservative and shall represent a pulsed operation of future fusion reactors [10]. Consequently, it takes about 30 s and 60 s for heating and cooling the samples between 300 °C and 550 °C, respectively (Figure 3). Even shorter heating duration could be achieved by higher heating power, but at an increased risk of overshooting the desired maximum temperature. On the other hand, the cooling duration becomes not significantly shorter when using volume streams of up to 20 l/min.

In regard to temperature differences between the two thermocouples in case of one coated sample, the temperature at the central thermocouple during heating up can be ≤ 7 °C higher than at the substrate/coating interface due to the induction field. When approaching the maximum temperature, the temperature difference becomes quickly ≈ 1 °C in less than 5 s (Figure 3). In case two samples are tested at the same time, each thermocouple is attached to one corresponding

7

substrate/coating interface and their temperatures differ at 300 and 550 °C about 4 and 8 °C from each other, respectively. Before and after the tests the temperature differences between the thermocouples are generally in the range of 0.5 °C and less.
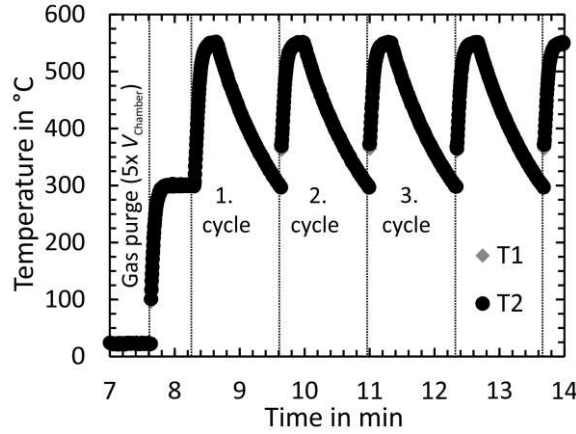

Figure 3. First thermal cycles of a sample of layer system 1 tested for 250 cycles.

For the thermal fatigue experiments in this test campaign, the samples were placed individually in the testing chamber, after attaching the thermo-wires, to assure that the lower and upper temperatures are exactly met. Then the thermocouples were connected to their feedthroughs, the lid closed and the gas volume exchanged. Subsequently, the samples were preheated to the minimum temperature and held for 20 s and then tested for the specified amount of thermal cycles. Finally, the samples were cooled to room temperature by Ar.

After the thermal fatigue tests, the samples were cut along their longitudinal axis by electrical discharge machining, embedded in resin and their cross-sections prepared by standard metallographic means. The cross-sections were analyzed in regard to their microstructure by scanning electron microscopy and measuring the microhardness profiles of the substrate. The microstructures were additional evaluated by electron backscatter diffraction (EBSD) analyses with the software CrystAlign from the ESPRIT suite [11], and also used for the determination of the average grain size. For the grain size analyses, an area of about 4000 µm² was scanned with a step

8

size of 0.1 µm, a lower and upper grain size limit of 0.5 µm and 8 µm were chosen, respectively, while a maximum misorientation for a grain of 5 ° was assumed. Furthermore, an area fraction weighting of the grain size was performed, whereas incomplete grains at the edges of the analyzed area were excluded in the calculation. This approach will rather lead to larger grain sizes and thus avoid an underestimation in case of lower analyses quality. In regard to the hardness profiles measurements, they were determined along two lines perpendicular to the coating/substrate interface using a Vickers indenter with a load of 9.81 N (HV1) and a minimum step size of 0.5 mm. Evolutionary changes in the hardness profiles would indicate that micro-mechanical processes, like creep, occur in the substrate during thermal cycling.

3. Results and Discussion

3.1. Microstructural and hardness analysis

After every thermal cycling test all coatings of the four layer system still adhered to their substrates. Furthermore, the microstructural analysis of the cross-section revealed also no crack initiation from the sample edges, no deterioration of the substrate/coating interface or of the coating itself, in form of detachments or formation of W/Fe intermetallic compounds, as exemplary depicted for layer system 1 in Figure 4. Hence, the layer systems are stable under the applied thermal loads.
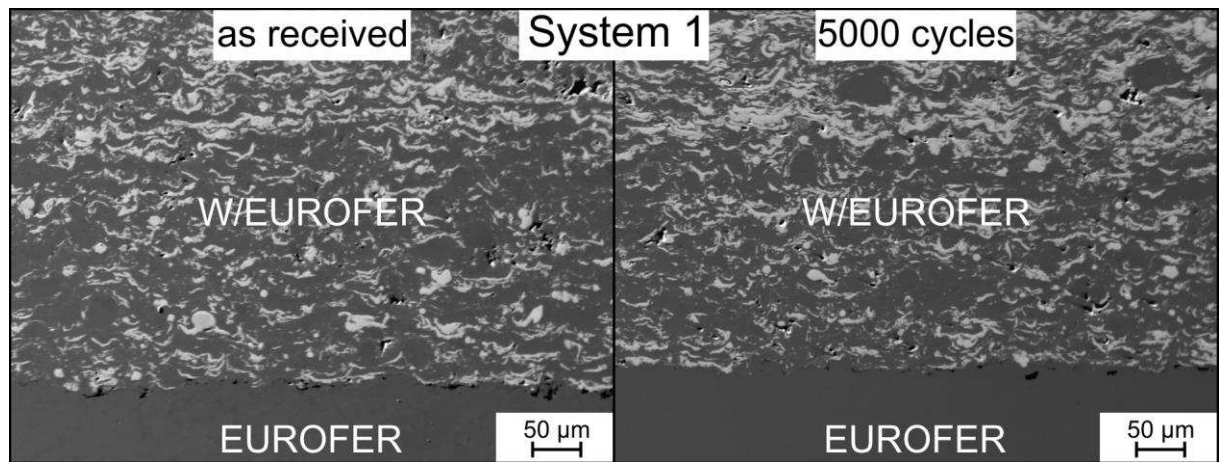
Figure 4. Substrate/coating interface of layer system 1 in the as-received state after coating and after 5000 thermal cycles.

In regard to the substrate hardness profiles (Figure 5), layer system 2 shows no change, whereas the other layer systems display no indicative evolution over the number of thermal cycles, although, layer system 1 and 3 exhibit a significant scatter in their hardness profiles, which reduces the detectability of possible changes. Furthermore, some hardness profiles of layer system 3 and, in particular, of layer system 1 show an increase in hardness, which requires further clarification. Nonetheless, due to the absence of an evolution over thermal cycles and due to the large scatter in the substrate hardness profiles, it is likely that the layer system properties are determined by the coating process and not influenced by thermal cycling.
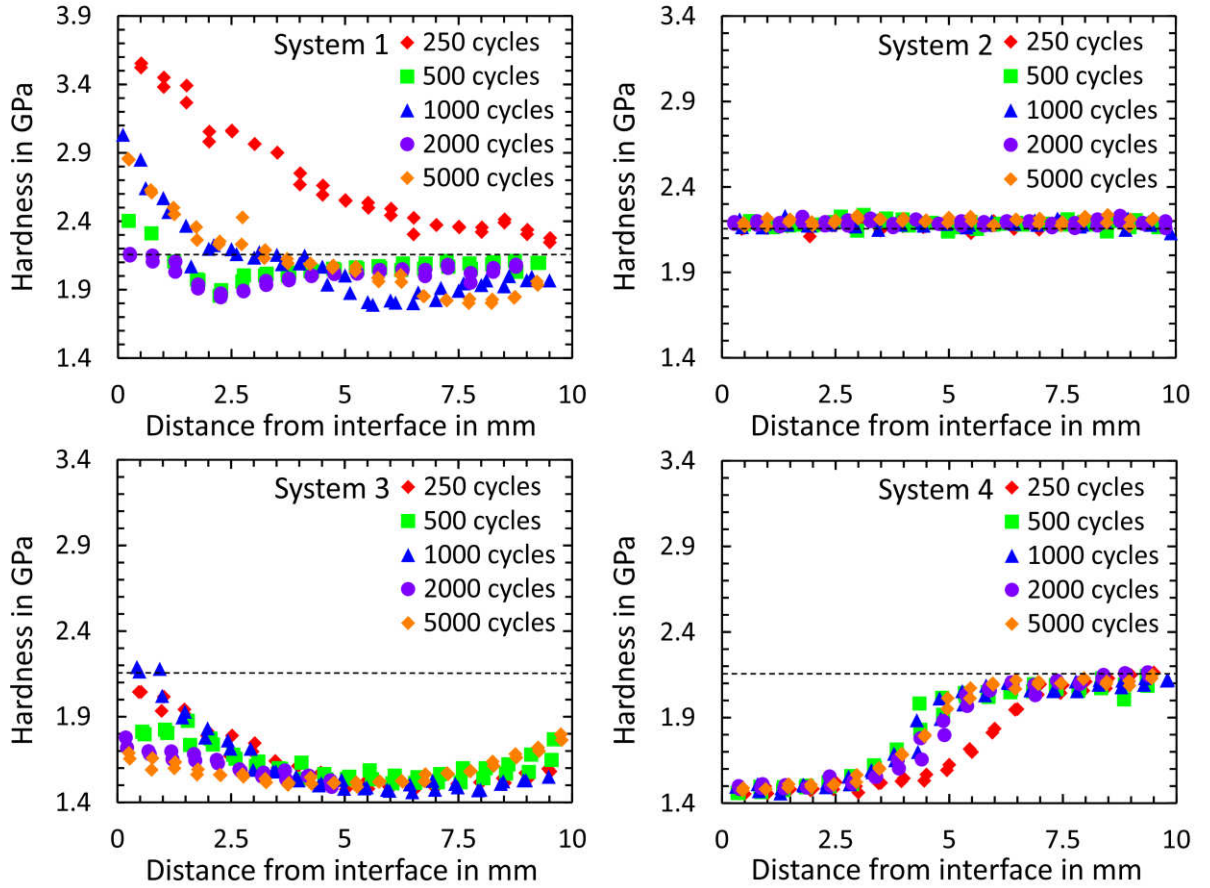
Figure 5. Substrate hardness profiles of the four layer systems after thermal cycling, with the nominal hardness of EUROFER marked by the dashed line.

To confirm, whether grain growth has also occurred in the sample areas with reduced hardness [3], and to clarify the effect for the areas with hardness increase EBSD analyses were performed.

3.2. EBSD analysis

The inverse pole figures (IPF) of the layer systems substrates after coating are depicted in Figure 6. For the base material, which shall be at a distance of 10 mm from the coating/substrate interface, the substrates exhibit, except for layer system 3, still a FM-structure. Near the interface, on the other hand, the layer systems have, apart from layer system 2, only a ferritic microstructure. These microstructures confirm that in areas with a reduced hardness recrystallization and grain growth occurred, because the tempering temperature of the substrate was exceeded during coating.
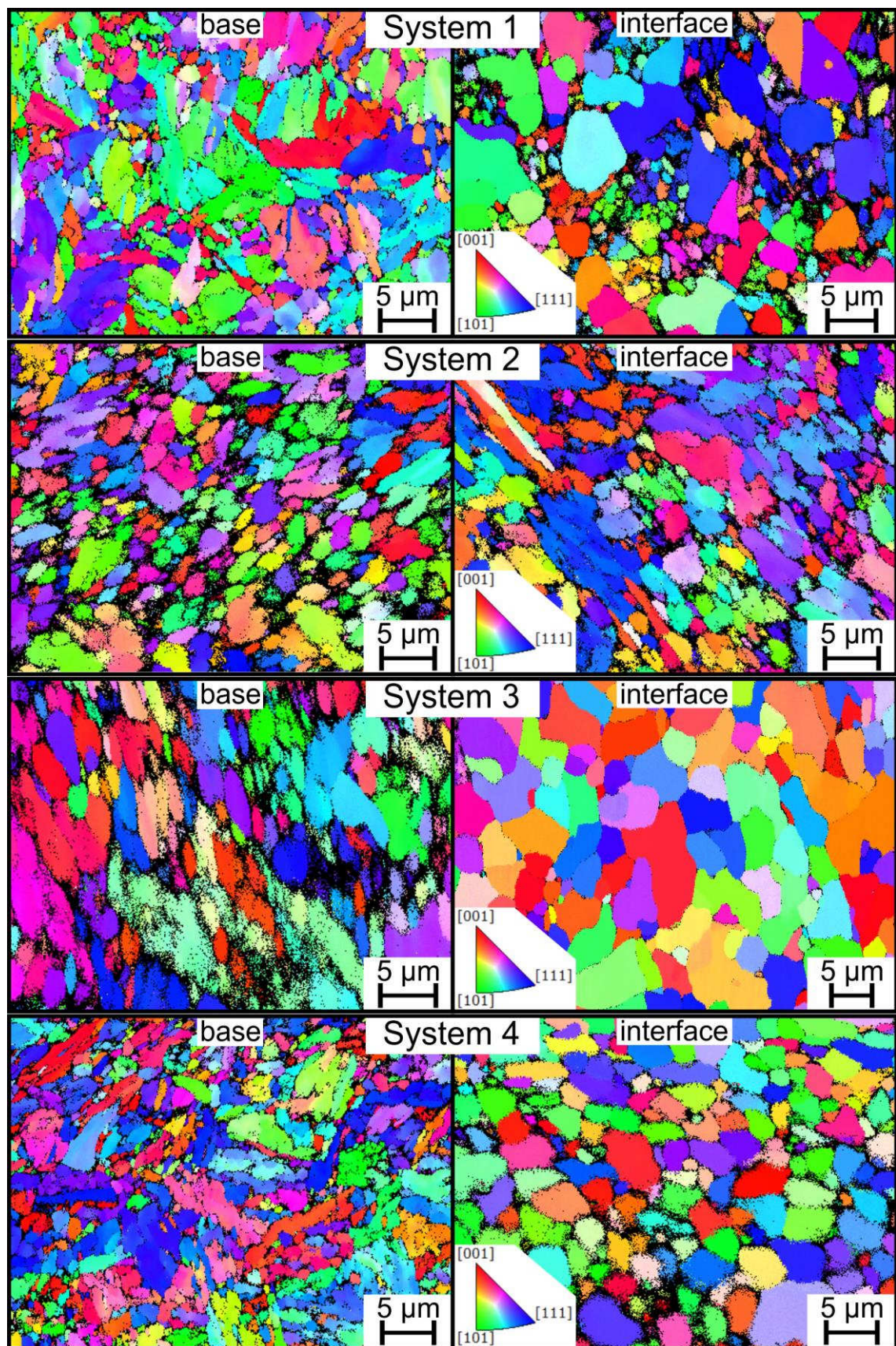
11

Figure 6. IPF of the layer systems substrates after coating, at a distance of about 10 mm from the coating/substrate interface (base) and close to the interface.
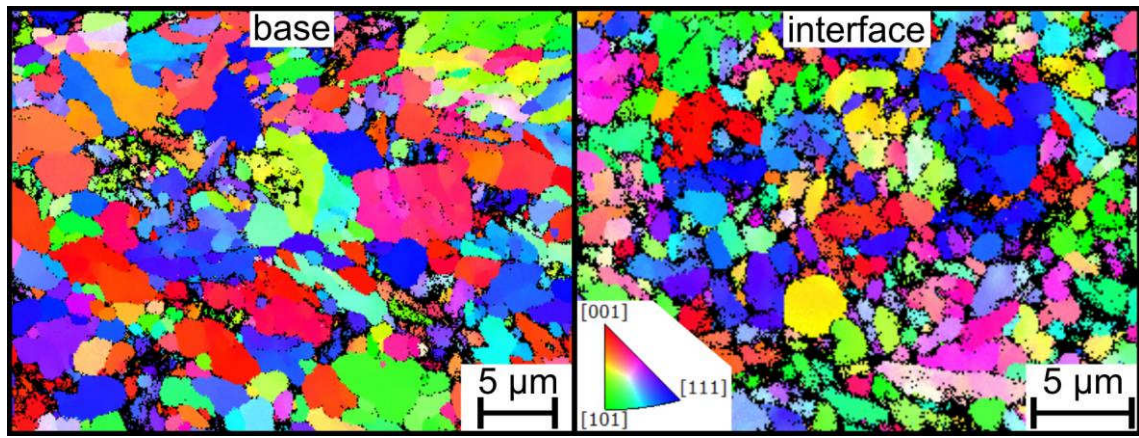
Figure 7. IPF of the substrate of layer system 1 tested for 250 thermal cycles, at a distance of about 10 mm from the coating/substrate interface (base) and close to the interface.

In case of the samples of layer system 1 that exhibit a higher hardness close to the interface, particularly the samples tested for 250 and 5000 cycles (Figure 5), a much finer microstructure is observed compared to the as-received state. This observation is corroborated by the determined average grain sizes, listed in Table 2. Furthermore, the measurements show that especially for these two samples the grains at the interface are also smaller than in their base material, and are therefore likely related to the hardness increase.

Table 2. Overview of the determined grain sizes.

Layer System	Cycle number	Grain size at interface in µm	Grain size at base in µm
	0	4.62	3.18
1	250	2.31	3.40
	5000	2.27	3.52
	0	3.73	3.57
2	5000	2.95	3.65
	0	5.18	4.04
3	5000	4.61	3.51
	0	4.52	3.34
4	5000	4.53	3.60

To achieve of a finer grain structure several options exist: Mechanical work with subsequent recrystallization annealing, normalizing, or due to compressive stresses that suppress grain growth

during recrystallization. The first option can be excluded and also the last one, as previous simulations [1] indicate tensile residual stresses inside the substrate.

Hence, it needs to be clarified in which way a normalizing like temperature sequence could occur during coating. The technical literature reports for the ferrite-austenite transition temperatures Ac_{1b} and Ac_{1e} of EUROFER 97 (heat E83699) temperatures of about 820 °C and 890 °C [12], respectively. In view of the samples, a transition from FM to ferritic microstructure has taken place in most layer systems. Therefore, it is presumed that the substrate temperature near the interface is at least 760 °C and consequently the temperature difference to the first transition temperature amounts to only about 60 °C. Furthermore, the material near the interface will quickly cool down, as soon as the spraying plasma plume has moved away or after the coating process, because of the three-dimensional heat transfer to the base material. The existence of such temperature gradient is confirmed by the FM-structure of the base material, indicating that the temperature was clearly below 760 °C at a distance of about 10 mm from the interface.

Following this line of thoughts, the material near the interface could have transformed partially into austenite during coating and then into martensite during cooling. Martensite seems a more likely cause for the measured hardness increase than only a refinement of the grain structure. For martensite formation fast quenching is not necessary, but can even be achieved with long cooling durations, as shown in the literature [12]: After complete austenitization at 980 °C for 20 min, the samples still formed predominantly martensite even with cooling durations of 4 h to room temperature [12]. Furthermore, the literature reports also the Vickers hardness values (HV10) after complete austenitization and quenching, for instance with 2, 300 and 3600 s duration, of 421 (4.13 GPa), 413 (4.05 GPa) and 390 (3.83 GPa), respectively [12], which are comparable to the high hardness values of the particular samples from layer system 1 (Figure 5).

Another approach to confirm the martensite based hardness increase would be to temper the respective samples and recover the material properties. For this, the sample of layer system 1 tested for 250 cycles was subjected to a heat treatment at about 760 °C for 90 min in a vacuum furnace and furnace cooling to room temperature. The afterwards determined hardness profile is compared to the previous one in Figure 8. On the one hand the hardness near the interface is clearly reduced and below the nominal hardness. On the other hand, the hardness difference between the interface near region and the base region is also significantly decreased. In case of the latter, the hardness lies, though, also below the nominal, but still above of the hardness reduced regions of layer systems 3 and 4 (Figure 5). From these observations it follows that martensite formation has very likely occurred during coating of layer system 1. That the hardness of the sample lies now generally below the nominal hardness could be due to the only partial martensitic transformation and remaining recrystallized ferritic grains. It shall be noted at this point that, although the temperatures were clearly above 800 °C, no Fe/W intermetallic compounds precipitated during coating, thus underlining the layer systems thermal stability [13].
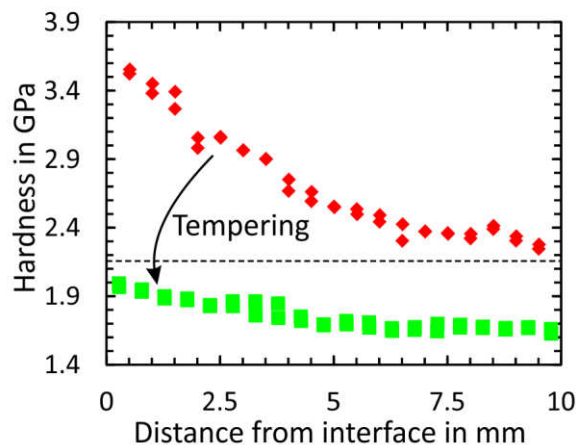

Figure 8. Hardness profile of the sample of layer system 1 tested for 250 thermal cycles before and after tempering.

In regard to the other samples of layer system 1, with lesser hardness increases, it is presumed that also martensite has formed. The possibility that the lesser hardness increase is due to

15

a too slow cooling, can be ruled out, because of the long, allowable quenching times for martensite formation [12]. The lesser hardness increase could, on the other hand, potentially result from a lower amount of martensite. This is, for instance, reflected by the large grains visible in the IPF of layer system 1 (Figure 6), implying that mainly grain growth took place. Consequently, a temperature difference must have existed between the areas with low and high hardness increase. Such a temperature difference could develop in the substrate plate during coating between its central area and edges, because the central area may not only receive heat from the spraying plasma but also from its surrounding regions. This heat accumulation is then sufficient for a significant ferrite-austenite transformation, contrarily to the edges.

In case of sample systems 3 and 4, predominantly loss of hardness and grain growth were observed, so that during coating the temperature was mainly still below the ferrite-austenite transition temperature. These two layer systems have thinner coatings than system 1 and were thus exposed for a shorter time to the spraying process. As a result, the samples did not receive the required amount of heat to reach the transition temperature like layer system 1.

In view of future components a very small and localized hardness loss, better than layer system 4, may be acceptable or could even be advantageous, as higher temperatures promote metallurgical bonding between coating and substrate. Complete recrystallization and ferrite formation, on the other hand, should be completely avoided, because then a complete hardening procedure, with temperatures that allow the formation of Fe/W intermetallic compounds, would be necessary. Also martensite formation needs to be prevented, as otherwise recrystallization will occur as well, due to temperature gradients. Achieving an ideal temperature distribution in components is subject of present, parallel work and will be published in the near future.

In regard to possible, but very small deterioration processes occurring during thermal cycling, based on simulations [1], they are obscured by the scatter in materials properties of the samples in this work. To detect such small changes, the samples could be characterized before and

after testing by suitable, non-destructive, high resolution techniques, and ideally source material with much more homogeneous properties should be used.

4. Conclusions and Outlook

From the presented investigations following conclusions can be drawn:

1. The four tested, functionally graded W/EUROFER layer systems are stable under the applied loads for at least 5000 thermal cycles between 300 and 550 °C.

2. The layer systems microstructural and hardness properties are determined by their coating processes and not influenced by thermal cycling.

3. The different substrate hardness profiles of these layer systems result from the specific coating processes: Hardness loss, due to recrystallization and grain growth, when the substrate tempering temperature was exceeded; Hardness increase, when even the ferrite-austenite transition temperature was exceeded, causing austenite formation during coating and martensite afterwards.

In future work the temperature range shall be further extended towards room temperature, so that also shut down scenarios of future fusion reactors can be analyzed. It is also of interest, whether very small deterioration processes can be detected with adequate precision, to verify previous simulations and further characterize the layer systems behavior.

References

[1] D.D. Qu, W.W. Basuki, J. Aktaa, Numerical assessment of functionally graded tungsten/EUROFER coating system for first wall applications, Fusion Eng. Des. 98-99 (2015) 1389–1393. https://doi.org/10.1016/j.fusengdes.2015.06.120.

[2] D.D. Qu, W.W. Basuki, J. Gibmeier, R. Vaßen, J. Aktaa, Development of Functionally Graded Tungsten/EUROFER Coating System for First Wall Application, Fusion Sci. Technol. 68 (3) (2015) 578–581. https://doi.org/10.13182/FST15-113.

[3] D. Qu, Development of functionally graded tungsten/EUROFER coating systems. PhD Thesis, Karlsruhe, 2016.

[4] J. Aktaa, D.D. Qu, Spraying 2 mm thick coating system and optimising the spray parameters. EUROfusion IDM EFDA_D_2MLW4C, 2016.

[5] T. Emmerich, D.D. Qu, R. Vaßen, J. Aktaa, Development of W-coating with functionally graded W/EUROFER-layers for protection of First-Wall materials, Fusion Eng. Des. 128 (2018) 58–67. https://doi.org/10.1016/j.fusengdes.2018.01.047.

[6] H. Bolt, V. Barabash, G. Federici, J. Linke, A. Loarte, J. Roth, K. Sato, Plasma facing and high heat flux materials - needs for ITER and beyond, J. Nucl. Mater. 307 (2002) 43–52.

[7] R. Vaßen, K.-H. Rauwald, O. Guillon, J. Aktaa, T. Weber, H.C. Back, D. Qu, J. Gibmeier, Vacuum plasma spraying of functionally graded tungsten/EUROFER97 coatings for fusion applications, Fusion Eng. Des. 133 (2018) 148–156. https://doi.org/10.1016/j.fusengdes.2018.06.006.

[8] T. Emmerich, J. Aktaa, Study to determine parameters for future design and fabrication rules of sacrificial W coatings. EUROfusion IDM EFDA_D_2NJ5R9, 2018.

[9] F. Arbeiter, C. Bachmann, Y. Chen, M. Ilić, F. Schwab, B. Sieglin, R. Wenninger, Thermal-hydraulics of helium cooled First Wall channels and scoping investigations on performance

improvement by application of ribs and mixing devices, Fusion Eng. Des. 109-111 (2016) 1123–1129. https://doi.org/10.1016/j.fusengdes.2016.01.008.

[10] G. Federici, C. Bachmann, L. Barucca, W. Biel, L. Boccaccini, R. Brown, C. Bustreo, S. Ciattaglia, F. Cismondi, M. Coleman, V. Corato, C. Day, E. Diegele, U. Fischer, T. Franke, C. Gliss, A. Ibarra, R. Kembleton, A. Loving, F. Maviglia, B. Meszaros, G. Pintsuk, N. Taylor, M.Q. Tran, C. Vorpahl, R. Wenninger, J.H. You, DEMO design activity in Europe: Progress and updates, Fusion Eng. Des. 136 (2018) 729–741. https://doi.org/10.1016/j.fusengdes.2018.04.001.

[11] Bruker Nano GmbH, ESPRIT (1.9.4.4) software suite: CrystAlign, Berlin.

[12] M. Rieth, M. Schirra, A. Falkenstein, P. Graf, S. Heger, H. Kempe, R. Lindau, H. Zimmermann, EUROFER 97: Tensile, Charpy, Creep and Structural Tests. FZKA 6911, Karlsruhe, 2003.

[13] T. Weber, M. Stüber, S. Ulrich, R. Vaßen, W.W. Basuki, J. Lohmiller, W. Sittel, J. Aktaa, Functionally graded vacuum plasma sprayed and magnetron sputtered tungsten/EUROFER97 interlayers for joints in helium-cooled divertor components, J. Nucl. Mater. 436 (1-3) (2013) 29–39. https://doi.org/10.1016/j.jnucmat.2013.01.286.